A Gas Proportional Scintillation Counter with krypton filling

Jinst

Published by IOP Publishing for Sissa Medialab

Received: *September 30, 2016*
Accepted: *December 7, 2016*
Published: *December 28, 2016*

18th International Workshop on Radiation Imaging Detectors
3–7 July 2016,
Barcelona, Spain

A Gas Proportional Scintillation Counter with krypton filling

C.M.B. Monteiro,[1] **R.D.P. Mano, E.C.G.M. Barata, L.M.P. Fernandes and E.D.C. Freitas**

LIBPhys, Physics Department, University of Coimbra,
Rua Larga, 3004-516 Coimbra, Portugal

E-mail: cristina@gian.fis.uc.pt

Abstract: A Gas Proportional Scintillation Counter filled with pure krypton was studied. Energy resolution below 10% for 5.9-keV X-rays was obtained with this prototype. This value is much better than the energy resolution obtained with proportional counters or other MPGDs with krypton filling. The krypton electroluminescence scintillation and ionisation thresholds were found to be about 0.5 and 3.5 kV $cm^{-1}bar^{-1}$, respectively.

Keywords: Gaseous detectors; X-ray detectors; Charge transport, multiplication and electroluminescence in rare gases and liquids

[1]Corresponding author.

doi:10.1088/1748-0221/11/12/C12079

Contents

2016 JINST 11 C12079

1 Introduction

Gaseous radiation detectors are highly adequate for X-ray spectrometry. However, while common solid-state X-ray detectors present energy resolutions around 150 eV for 6 keV, the commonly used proportional counter may reach energy resolutions of about 800 eV. In addition, modern gaseous detectors based on hole-type structures for signal (charge) amplification may present even worse energy resolutions. Nevertheless, gaseous detectors present advantages over the solid-state ones, such as room temperature operation and large detection areas with low-cost 2D-imaging capabilities.

Gas Proportional Scintillation Counters (GPSC) are X-ray gaseous detectors where the charge signal produced by the X-ray interaction is amplified through gas secondary scintillation processes produced by electron impact, the so-called electroluminescence (EL) [1], in opposition to the charge avalanche amplification processes commonly used in gaseous detectors. In gaseous detectors, the electrons produced in the radiation interaction with the gas medium are driven towards a region where the electric field is large enough to promote signal amplification. For GPSCs, the applied electric field is only high enough to excite but not ionise the noble gas atoms, producing a scintillation pulse through the atom's de-excitation. This electroluminescence is proportional to the number of electrons produced in the interaction. As the statistical fluctuations inherent to the scintillation process are much less than those associated to the avalanche ionisation processes and less than those associated to the charge produced by the X-ray interactions, GPSCs may reach energy resolutions around 450 eV for 6 keV X-rays. On the other hand, the need for a photosensor and the requirement for a very pure noble gas filling [2] presented a drawback in the use of GPSCs. Therefore, they have only been used in specific applications, mostly X-ray astrophysics [3–5], and only one commercial application has been implemented [6] for X-ray spectrometry. With the development of dual-phase noble gas time-projection chambers (TPCs) for direct dark matter search [7–9] and, recently, the development of high-pressure xenon TPCs for double-beta decay detection [10, 11] and for directional dark matter search [12, 13], the EL amplification concept has been applied again.

The application of GPSCs has been limited, mostly due to the use of vacuum photomultiplier tubes (PMT) for the scintillation readout. These photosensors are fragile, bulky and power consuming devices. Alternative gaseous photosensors based on CsI-coated microstrip plates have been implemented [14–16], as well as multi-alkali photocathode based vacuum photocells [17]. However,

solid-state large area avalanche photodiodes (LAAPD), developed in the last two decades, and the recently developed silicon-photomultipliers (SiPMs), pixelized avalanche photodiodes operating in Geiger mode, present an actual significant alternative to PMTs [18–21]. In addition, solid-state photosensors allow building large-area, yet compact, low power-consuming and cost-effective photosensor readouts with 2D-imaging capabilities [22, 23]. It is possible, thus, to have a competitive GPSC for spectrometry applications, where a large detection area and/or imaging capability are important assets [22].

Xenon and argon are the most studied filling gases due to their use in rare event detection, e.g. WIMP dark matter and neutrinoless double-beta decay search [7–13, 24–26]. EL yield has been determined in Xe and Ar for uniform electric fields [27–31] as well as for electron avalanches in GEM and THGEM [32], MicroMegas [33] and MHSP based detectors [34, 35]. While Xe GPSCs present energy resolutions a factor of two lower than those achieved with Xe-based proportional counters and micropattern detectors, Ar GPSCs present similar energy resolutions to those based on electron multiplication.

Krypton has a radioactive isotope, which disfavours its use in rare-event applications. Nevertheless, Kr is denser than Ar, much more inexpensive and presents even the highest absorption cross section for X-rays in the 14–34 keV energy range when compared to xenon. These are advantages when large detection volumes and/or high-pressure are requirements and in specific applications where its natural radioactivity background will not seriously affect its operation due to the high intensity of incident radiation, like in some x- and gamma-ray spectrometry applications, or the possibility of efficient background discrimination in rare-event detection [36–39]. Kr detectors have been already proposed for double-beta decay and double electron-capture detection [37–39].

In this work, we present studies on a Kr-filled GPSC, using a large-area avalanche photodiode as photosensor. The performance obtained in terms of electroluminescence and energy resolution will be presented with some examples of its X-ray spectrometry capabilities.

2 Experimental setup

The gas proportional scintillation counter used for these studies integrates a large area avalanche photodiode from Advanced Photonics, Inc. as the VUV photosensor [20]. The detector is depicted schematically in figure 1 and was used in previous works [18, 19, 28]. For the present studies, the used filling gas is krypton.

The GPSC enclosure is a stainless steel cylinder with 10 cm in diameter and 5 cm in height. It is a standard, uniform field type GPSC with a 2.5-cm thick drift/absorption region and a 0.9-cm thick scintillation region. This region is limited by two grids, G1 and G2, which are made of highly transparent stainless steel 80-μm diameter wires with 900 μm spacing. The detector radiation window is made of aluminized Melinex, 6-μm thick and 2-mm in diameter. A Macor piece insulates the holders of both radiation window and grid G1. A low vapour pressure epoxy was used to vacuum-seal the Macor piece, the radiation window and holder as well as the voltage feedthrough of grid G1. The LAAPD was placed just below the second grid, G2, and was vacuum-sealed by compressing the photodiode enclosure against the stainless steel detector body using an indium ring. The GPSC was vacuum pumped to pressures below 10^{-5} mbar and, then, filled with

2016 JINST 11 C12079

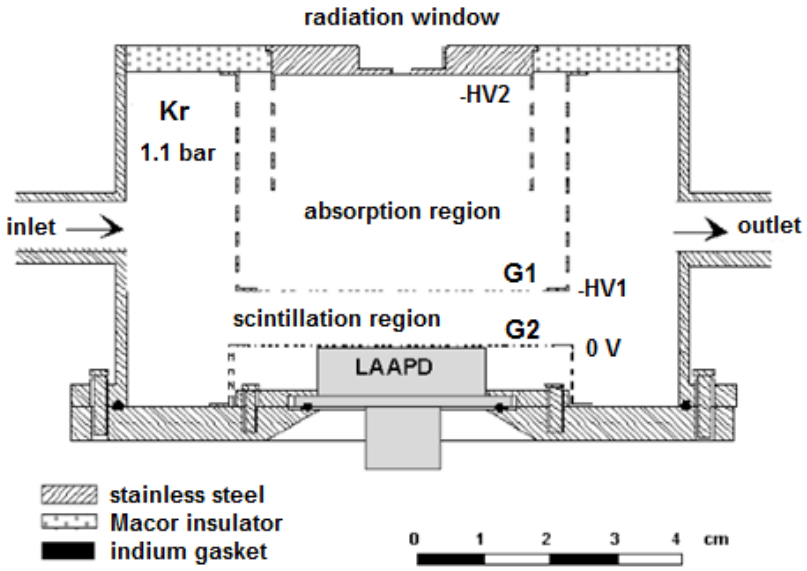

Figure 1. Schematic of the GPSC equipped with a large area avalanche photodiode (LAAPD) as the VUV photosensor.

krypton at a pressure of 1.1 bar. The gas was continuously purified by convection through St707 SAES getters [17], which were set to a stable temperature of about 150°C.

The GPSC radiation window and its focusing electrode were operated at negative voltage, as well as mesh G1 and respective holder, while mesh G2, its holder and the LAAPD enclosure were maintained at 0 V. The voltage difference between the radiation window and grid G1 determines the reduced electric field E/p — the electric field intensity divided by the gas pressure — in the absorption region, while the voltage applied to grid G1 determines the reduced electric field in the scintillation region. The LAAPD is a deep-UV enhanced series from Advanced Photonix Inc., with 16 mm active diameter, and was biased at 1840 V, corresponding to a gain of approximately 150.

The LAAPD signals were fed through a low-noise, 1 V/pC charge sensitive pre-amplifier (Canberra 2006) to a Tennelec TC 243 linear amplifier with 2-μs shaping time constants, and were pulse-height analysed with a Nucleus PCA-II multi-channel analyser (MCA).

3 Experimental results

The detector was irradiated with X-rays from a ^{55}Fe radioactive source, collimated to a diameter of 1.5 mm. Figure 2 depicts a typical pulse-height distribution obtained for these studies. The spectral features comprise the peak resulting from Kr electroluminescence collected in the LAAPD, the peak resulting from the direct interaction of 5.9 keV X-rays in the LAAPD, and the electronic noise tail in the low-energy limit. In the scintillation peak, the Mn K_α (5.9 keV) and K_β (6.4 keV) lines are overlapped. For better analysis of the response to 5.9 keV X-rays, the Mn K_β-line was efficiently eliminated by means of a chromium film placed in front of the radiation window.

2016 JINST 11 C12079

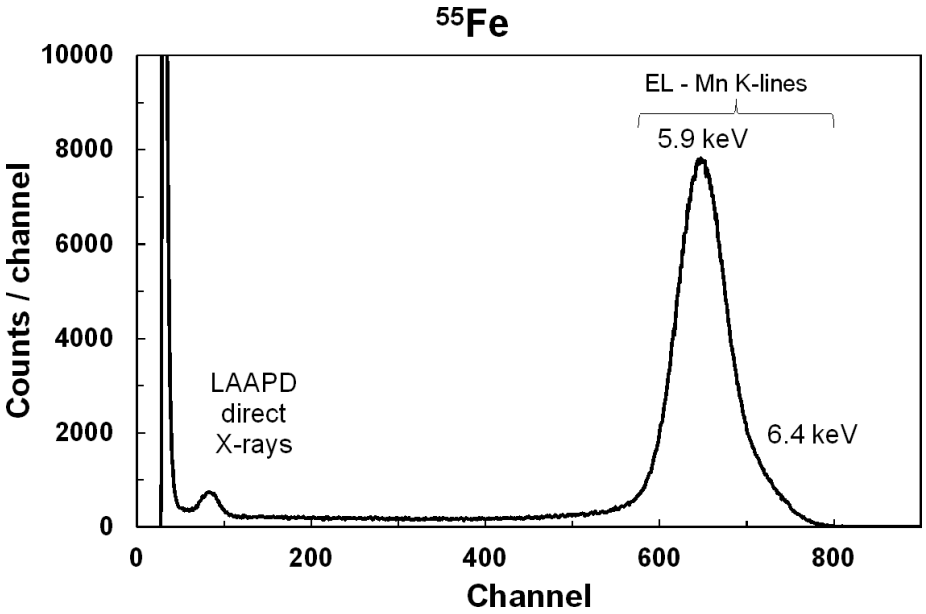

Figure 2. Typical pulse-height distribution obtained for the ^{55}Fe X-ray source, with the krypton-GPSC instrumented with a LAAPD as VUV photosensor, for E/p values of 0.34 and 3.4 kV cm^{1} bar^{-1} in the drift and scintillation regions, respectively. The LAAPD was operated at a gain of approximately 150. The scintillation peak shows X-rays from both Mn K_α and K_β line X-rays.

For pulse amplitude and energy resolution measurements, the pulse-height distributions were fit to Gaussian functions superimposed on a linear background, from which the Gaussian centroid — relative amplitude — and relative FWHM — energy resolution — were determined. In the case of figure 2, the count rate for 5.9 keV X-ray pulses resulting from interactions in the gas and directly in the LAAPD was about 900 and 20 Hz, respectively. The pulse-height distribution exhibits a very low background level in the regions outside the peaks, with a peak-to-valley ratio above 50 for the electroluminescence peak.

The amplitude of the scintillation peak depends on the voltage applied to the GSPC scintillation region as well as on the LAAPD bias voltage. As for the amplitude of the events resulting from direct X-ray interactions in the LAAPD, it depends only on the voltage applied to the LAAPD. In addition, the events ensuing direct interaction in the LAAPD are visible even when the electric field applied to the scintillation region is zero.

The focusing electrode and the G1-holder electrode do not produce a uniform electric field in the drift region, resulting in a significant dependence of both pulse amplitude and energy resolution on the voltage difference applied across the drift region, i.e. between the radiation window and grid G1. Figure 3 presents the detector relative amplitude and energy resolution for 5.9 keV X-rays as a function of reduced electric field in the drift region, for a reduced electric field of 3.4 kV cm^{-1} bar^{-1} in the scintillation region. As the drift electric field decreases, the pulse amplitude also decreases and the energy resolution degrades. This is due to the loss of primary electrons to recombination with ions in the gas medium for X-ray interactions in regions close to the detector window, as a result of the very low electric field present in this region. For the present detector geometry, optimum values for the energy resolution are obtained for drift E/p values around 0.4 kV cm^{-1} bar^{-1}.

2016 JINST 11 C12079

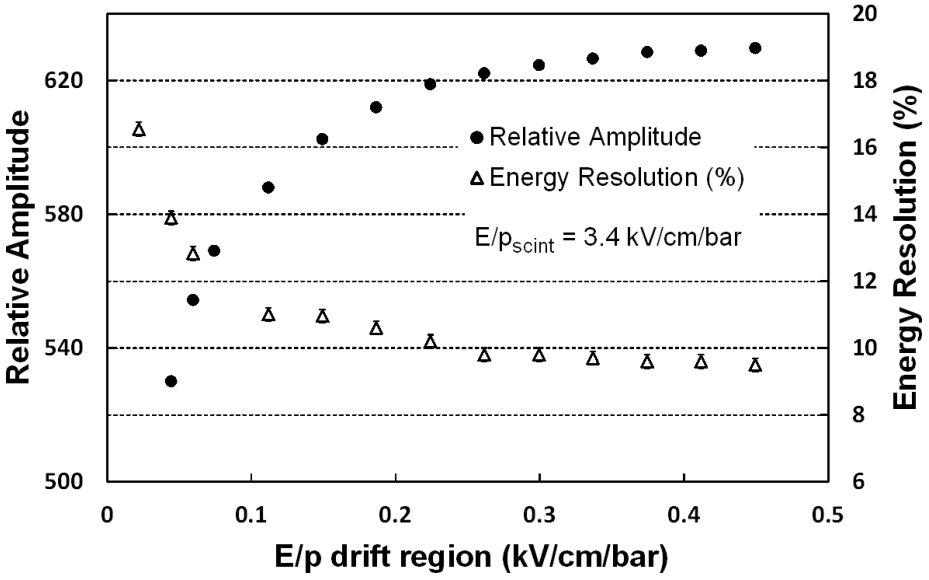

Figure 3. GPSC relative pulse amplitude as a function of reduced electric field in the drift region. The reduced electric field in the scintillation region and the LAAPD bias voltage were kept constant throughout the measurements.

Figure 4 depicts the detector relative amplitude as a function of reduced electric field in the scintillation region, for an E/p value of 0.4 kV cm^{-1} bar^{-1} in the drift region. The results follow the typical behaviour of electroluminescence in noble gases, i.e. an approximately linear dependence on the reduced electric field in the scintillation region, with the scintillation threshold at an E/p value of about 0.5 kV cm^{-1} bar^{-1} for krypton. This value is in good agreement with other data obtained by Monte Carlo simulations or Boltzmann numerical calculations [40, 41]. Above an E/p value of about 3.3 kV cm^{-1} bar^{-1}, the relative amplitude variation deviates from the linear behaviour, reflecting the exponential growth in the number of electrons present in the scintillation region due to the onset of the ionisation processes by electron impact. Energy resolutions (FWHM) below 10% can be achieved with the Kr-GPSC for 5.9-keV X-rays. This value is much better than those achieved with proportional counters or other MPGDs with Kr-filling. Comparing to Xe-filled GPSCs, the Kr-filling option presents a small degradation in the detector energy resolution, which can be tolerable in specific applications where the Kr lower cost, high absorption cross sections for X-rays in the 14–34 keV range and lower absorption cross section for low-energy X-rays are important assets.

Figure 5 presents pulse-height distributions obtained with this GPSC when irradiated by ^{241}Cm and ^{244}Am radioactive sources. Photon energies above the Kr K-absorption edge produce intense escape peaks, since the Kr K-fluorescence X-rays resulting from these photon interactions have a significant probability of escaping the drift region. Figures 2 and 5 clearly show that the natural radioactivity of Kr is sufficiently low to produce insignificant background in the considered energy regions for count rates as low as few 10^3 c/s. For higher X-ray energies, the pulse-height distribution deviates from the Gaussian response due to X-ray interactions in the scintillation region, which lead to lower electroluminescence output as the X-rays interacting deeper in the scintillation region produce only partial amplification when crossing the region.

2016 JINST 11 C12079

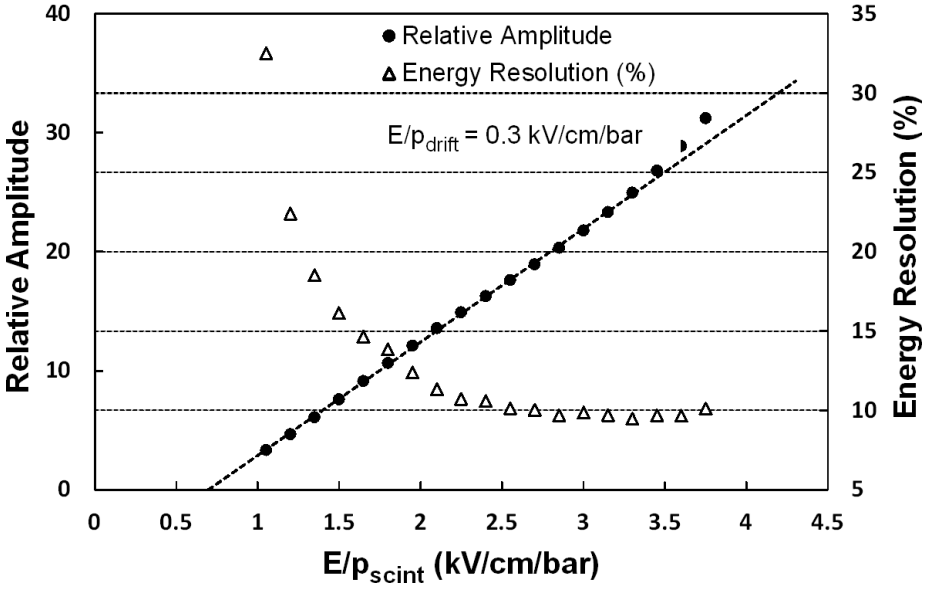

Figure 4. GPSC relative pulse amplitude as a function of reduced electric field in the scintillation region. The line presents the least square fit to the points below 3.3 V cm^{-1} bar^{-1}. The reduced electric field in the drift region and the LAAPD biasing were kept constant throughout the measurements.

4 Conclusions

We have investigated the performance of a Kr-filled GPSC, using a large-area avalanche photodiode as a VUV photosensor. Energy resolution values below 10% for 5.9 keV X-rays were obtained with our prototype, which is much better than those achieved with proportional counters or other MPGDs with Kr-filling. Comparing to Xe-filled GPSCs, the Kr- GPSC presents a small degradation in energy resolution, which can be tolerable in specific applications where the Kr lower cost, high absorption cross sections for X-rays in the 14–34 keV range and lower absorption cross section for low-energy X-rays are important assets.

The performance of the detector in terms of electroluminescence was also investigated. The results follow the typical behaviour of electroluminescence in noble gases, with a scintillation threshold, for krypton, at an E/p value of about 0.5 kV cm^{-1} bar^{-1}. This value is in good agreement with simulation and theoretical results. The ionisation threshold was found to be around 3.5 kV cm^{-1} bar^{-1}.

Finally, the capabilities of the Kr-GPSC for X-ray spectrometry were demonstrated through several energy spectra collected for radioactive sources with multiple X-ray lines.

Acknowledgments

This work is funded by FEDER, through the Programa Operacional Factores de Competitividade — COMPETE and by National funds through FCT — Fundação para a Ciência e Tecnologia in the frame of project PTDC/FIS/-NUC/1534/2014 and project UID/FIS/04559/2013 (LIBPhys). C.M.B. Monteiro and E.D.C. Freitas acknowledge FCT grants SFRH/BPD/76842/2011 and SFRH/BPD/109180/2015, respectively.

2016 JINST 11 C12079

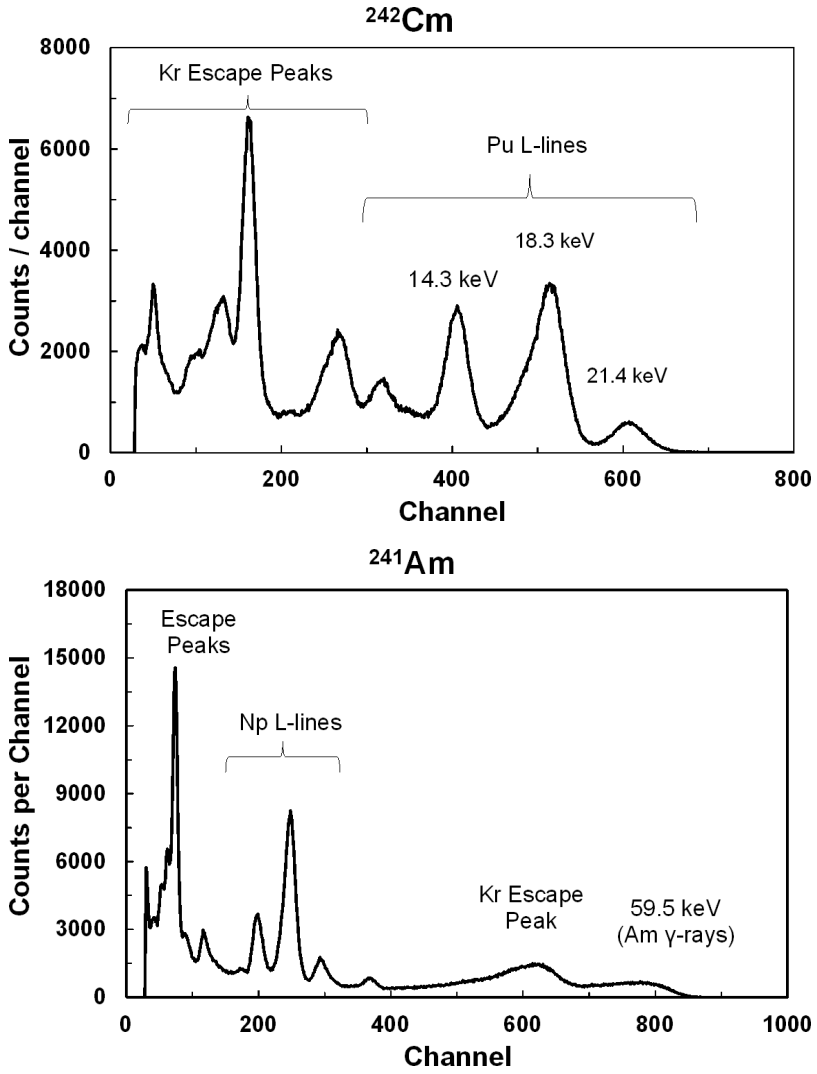

Figure 5. Pulse-height distributions obtained for ^{241}Cm and ^{244}Am X-rays and γ photons irradiating the krypton-GPSC instrumented with a LAAPD as VUV photosensor, for an E/p value of 3.4 kV cm^{1} bar^{-1} in the scintillation region. The LAAPD was operated at a gain of approximately 150.

References

[1] J.M.F. dos Santos, J.A.M. Lopes, J.F.C.A. Veloso et al., *Development of portable gas proportional scintillation counters for X-ray spectrometry*, *X-Ray Spectrom.* **30** (2001) 373.

[2] T. Himi et al., *Emission spectra from Ar-Xe, Ar-Kr, Ar-N_2, Ar-CH_4, Ar-CO_2 and Xe-N_2 gas proportional scintillation counters*, *Nucl. Instr. Meth.* **A 205** (1983) 591.

[3] A.N. Parmar et al., *The low-energy concentrator spectrometer on-board the BeppoSAX X-ray astronomy satellite*, *Astron. Astrophys. Suppl. Ser.* **122** (1997) 309.

[4] G. Fazio et al., *The on-ground calibration of the flight model of the HPGSPC onboard the SAX satellite: calibration set-up and preliminary results*, *Nuovo Cim.* **20** (1997) 819.

[5] R.A. Austin, B.D. Ramsey et al., *A high-pressure gas-scintillation-proportional counter for the focus of a hard-X-ray telescope*, *Proc. SPIE* **3765** (1999) 714.

[6] D.A. Goganov and A.A. Schultz, *A gas-filled electroluminescence detector for EDXRF spectrometry*, *X-Ray Spectrom.* **35** (2006) 47.

[7] ZEPLIN collaboration, T.J. Sumner, *The ZEPLIN III dark matter project*, *New Astron. Rev.* **49** (2005) 277.

[8] D.N. McKinsey et al., *The LUX Dark Matter Search*, *J. Phys. Conf. Ser.* **203** (2010) 012026.

[9] XENON100 collaboration, E. Aprile et al., *The XENON100 Dark Matter Experiment*, *Astropart. Phys.* **35** (2012) 573 [arXiv:1107.2155].

[10] NEXT collaboration, V. Alvarez et al., *NEXT-100 Technical Design Report (TDR): Executive Summary*, 2012 *JINST* **7** T06001 [arXiv:1202.0721].

[11] PANDAX-III collaboration, J. Galan, *Microbulk MicrOMEGAs for the search of $0\nu\beta\beta$ of ^{136}Xe in the PandaX-III experiment*, 2016 *JINST* **11** P04024 [arXiv:1512.09034].

[12] D. Nygren, *Columnar recombination: a tool for nuclear recoil directional sensitivity in a xenon-based direct detection WIMP search*, *J. Phys. Conf. Ser.* **460** (2013) 012006.

[13] G. Mohlabeng, K. Kong, J. Li, A. Para and J. Yoo, *Dark Matter Directionality Revisited with a High Pressure Xenon Gas Detector*, *JHEP* **07** (2015) 092 [arXiv:1503.03937].

[14] J.F.C.A. Veloso, J.M.F.dos Santos, C.A.N. Conde, *Gas proportional scintillation counters with a CsI-covered microstrip plate UV photosensor for high-resolution X-ray spectrometry*, *Nucl. Instr. Meth.* **A 457** (1983) 253.

[15] C.M.B. Monteiro et al., *The performance of the GPSC/MSGC hybrid detector with argon-xenon gas mixtures*, *IEEE Trans. Nucl. Sci.* **49** (2002) 907.

[16] C.M.B. Monteiro, J.F. C.A. Veloso, D.S. A.P. Freitas, J.M.F. dos Santos and C.A.N. Conde, *The gas proportional scintillation counter / microstrip gas chamber hybrid detector with argon filling*, *Nucl. Instrum. Meth.* **A 490** (2002) 169.

[17] A.D. Goganov et al., *Electroluminescence gas-filled detector with a build-in photocell*, *Nucl. Instr. Meth.* **A 603** (2009) 56.

[18] J.A.M. Lopes et al., *A xenon gas proportional scintillation counter with a UV-sensitive large-area avalanche photodiode*, *IEEE Trans. Nucl. Sci.* **48** (2001) 312.

[19] C.M.B. Monteiro et al., *An argon gas proportional scintillation counter with UV avalanche photodiode scintillation readout*, *IEEE Trans. Nucl. Sci.* 48 (2001) 1081.

[20] L.M.P. Fernandes et al., *Characterization of large area avalanche photodiodes in X-ray and VUV-light detection*, 2007 *JINST* **2** P08005 [physics/0702130].

[21] T. Lux, E.D.C. Freitas, F.D. Amaro, O. Ballester, G.V. Jover-Manas, C. Martin et al., *Characterization of the Hamamatsu S8664 Avalanche Photodiode for X-Ray and VUV-light detection*, *Nucl. Instrum. Meth.* **A 685** (2012) 11 [arXiv:1108.5143].

[22] T. Lux et al., *Development and Characterization of a Multi-APD Xenon Electroluminescence TPC*, 2015 *JINST* **10** P03008 [arXiv:1409.8636].

[23] NEXT collaboration, P. Ferrario et al., *First proof of topological signature in the high pressure xenon gas TPC with electroluminescence amplification for the NEXT experiment*, *JHEP* **01** (2016) 104 [arXiv:1507.05902].

2016 JINST 11 C12079

[24] A. Marchionni et al., *ArDM: a ton-scale LAr detector for direct Dark Matter searches*, *J. Phys. Conf. Ser.* **308** (2011) 012006.

[25] WARP R&D Group collaboration, P. Kryczynski, *Pulse Shape Discrimination in liquid argon and its implications for Dark Matter searches using depleted argon*, *Acta Phys. Polon.* **B 43** (2012) 1509 [arXiv:1210.1019].

[26] P.D. Meyers, *DarkSide-50: a WIMP search with a two-phase argon TPC*, *Physics Procedia* **61** (2015) 124.

[27] C.M.B. Monteiro, L.M.P. Fernandes, J.A.M. Lopes, L.C.C. Coelho, J.F. C.A. Veloso, J.M. F.d. Santos et al., *Secondary Scintillation Yield in Pure Xenon*, 2007 *JINST* **2** P05001 [physics/0702142].

[28] C.M.B. Monteiro, J.A.M. Lopes, J.F. C.A. Veloso and J.M.F. dos Santos, *Secondary scintillation yield in pure argon*, *Phys. Lett.* **B 668** (2008) 167.

[29] E.D.C. Freitas, C.M.B. Monteiro, M. Ball, J.J. Gomez-Cadenas, J.A.M. Lopes, T. Lux et al., *Secondary scintillation yield in high-pressure xenon gas for neutrinoless double beta decay (0nu beta beta) search*, *Phys. Lett.* **B 684** (2010) 205.

[30] L.M.P. Fernandes, E.D.C. Freitas, M. Ball, J.J. Gomez-Cadenas, C.M.B. Monteiro, N. Yahlali et al., *Primary and secondary scintillation measurements in a xenon Gas Proportional Scintillation Counter*, 2010 *JINST* **5** P09006 [*Erratum ibid.* **5** (2010) A12001] [arXiv:1009.2719].

[31] K. Kazkaz and T.H.Y. Joshi, *A Model for the Secondary Scintillation Pulse Shape from a Gas Proportional Scintillation Counter*, 2016 *JINST* **11** P03002 [arXiv:1512.05320].

[32] C.M.B. Monteiro, L.M.P. Fernandes, J.F. C.A. Veloso, C.A.B. Oliveira and J.M.F. dos Santos, *Secondary scintillation yield from GEM and THGEM gaseous electron multipliers for direct dark matter search*, *Phys. Lett.* **B 714** (2012) 18.

[33] C. Balan, E.D.C. Freitas, T. Papaevangelou, I. Giomataris, H.N. da Luz, C.M.B. Monteiro et al., *MicrOMEGAs operation in high pressure xenon: Charge and scintillation readout*, 2011 *JINST* **6** P02006 [arXiv:1009.2960].

[34] J.M. Maia et al., *Advances in the Micro-Hole & Strip Plate gaseous detector*, *Nucl. Instr. Meth.* **A 504** (2004) 364.

[35] C.M.B. Monteiro et al., *Secondary scintillation yield from gaseous micropattern electron multipliers in direct Dark Matter detection*, *Phys. Lett.* **B 667** (2009) 133.

[36] A. Buzulutskov, *Two-phase cryogenic avalanche detectors for astroparticle and medical imaging*, proposal for INTAS grant 04-78-6744 (2004).

[37] A. Bolozdynya et al., *An electroluminescence emission detector to search for double-beta positron decays of ^{124}Xe and of ^{78}Kr*, *IEEE Trans. Nucl. Sci.* **44** (1997) 1046.

[38] Yu.M. Gavrilyuk, A.M. Gangapshev, V.V. Kazalov, V.V. Kuzminov, S.I. Panasenko and S.S. Ratkevich, *Indications of 2v2K capture in 78Kr*, *Phys. Rev.* **C 87** (2013) 035501.

[39] S. Bustabad, G. Bollen, M. Brodeur, D.L. Lincoln, S.J. Novario, M. Redshaw et al., *Examination of the possible enhancement of neutrinoless double-electron capture in ^{78}Kr*, *Phys. Rev.* **C 88** (2013) 035502.

[40] M.A. Feio, A.J.P.L. Policarpo and M.A.F. Alves, *Thresholds for secondary light emission by noble gases*, *Jpn. J. Appl. Phys.* **21** (1982) 1184.

[41] T.H.V.T. Dias, A.D. Stauffer and C.A.N. Conde, *Unidimensional Monte Carlo simulation of electron drift velocities and electroluminescence in argon, krypton and xenon*, *J. Phys.* **D 19** (1986) 527.

2016 JINST 11 C12079